Supplementary material - Appendices

A A translating and rotating sphere in the two-fluid medium

For a sphere translating with a velocity $\boldsymbol{U}$ in a two-fluid medium, the dimensionless governing equations for the solvent and polymer phases are given by:

$$\nabla^2 \boldsymbol{u}_s - \nabla p_s - \frac{1}{L_B^2}(\boldsymbol{u}_s - \boldsymbol{u}_p) = 0 \tag{1}$$

$$\lambda \nabla^2 \boldsymbol{u}_p - \lambda \nabla p_p + \frac{1}{L_B^2}(\boldsymbol{u}_s - \boldsymbol{u}_p) = 0 \tag{2}$$

where, $\boldsymbol{u}_s, \boldsymbol{u}_p, p_s, p_p$ correspond to the solvent and polymer velocities and pressures respectively. Assuming solutions of the form

$$\boldsymbol{u}_s = \boldsymbol{f} \cdot (\nabla\nabla - \boldsymbol{I}\nabla^2) f_s(r) \tag{3}$$

$$p_s = \boldsymbol{f} \cdot \nabla h_s(r) \tag{4}$$

$$\boldsymbol{u}_p = \boldsymbol{f} \cdot (\nabla\nabla - \boldsymbol{I}\nabla^2) f_p(r) \tag{5}$$

$$p_p = \boldsymbol{f} \cdot \nabla h_p(r) \tag{6}$$

where $\boldsymbol{f} = \boldsymbol{U}$ for this case (but it can be an arbitrary vector that depends on the boundary condition in general), the governing equations reduce to,

$$\nabla^2 f_s - h_s - \frac{1}{L_B^2}(f_s - f_p) = 0 \tag{7}$$

$$\lambda \nabla^2 f_p - \lambda h_p + \frac{1}{L_B^2}(f_s - f_p) = 0 \tag{8}$$

$$\nabla^2 h_s = \lambda \nabla^2 h_p = 0 \tag{9}$$

These equations can be solved by defining a mixture flow $f_m = f_s + \lambda f_p$, $h_m = h_s + \lambda h_p$, and a difference flow $f_d = f_p - f_s$ and $h_d = h_p - h_s$ for which the equations reduce to,

$$\frac{1}{r^2}\frac{d}{dr}\left(r^2 \frac{df_m}{dr}\right) - h_m = 0 \tag{10}$$

$$\frac{1}{r^2}\frac{d}{dr}\left(r^2 \frac{df_d}{dr}\right) - \left(\frac{1+\lambda}{\lambda L_B^2}\right) f_d - h_d = 0 \tag{11}$$

which are the well-known Stokes' equation and the Brinkman equation respectively. Note that here and in Eq.7 and Eq.8, the Laplacian only involves the radial derivative owing to spherical symmetry in the problem. The boundary conditions used are:

$$\boldsymbol{u}_s, \boldsymbol{u}_p \to 0 \text{ as } r \to \infty \tag{12}$$

$$\boldsymbol{u}_p \cdot \boldsymbol{n} = \boldsymbol{U} \cdot \boldsymbol{n} \text{ at } r = a \tag{13}$$

$$\boldsymbol{u}_s = \boldsymbol{U} \text{ at } r = a \tag{14}$$

$$(\boldsymbol{I} - \boldsymbol{n}\boldsymbol{n}) \cdot (\boldsymbol{\sigma}_p \cdot \boldsymbol{n}) = 0 \text{ at } r = a \tag{15}$$

where the last boundary condition corresponds to zero polymeric tangential stress at the sphere's surface. Solving Eq.9 and Eq.10 subject to these BCs gives,

$$\boldsymbol{u}_s = k_1\ \boldsymbol{f} + k_2(\boldsymbol{f}\cdot\boldsymbol{n})\boldsymbol{n} \tag{16}$$

$$\boldsymbol{u}_p = k_3\ \boldsymbol{f} + k_4(\boldsymbol{f}\cdot\boldsymbol{n})\boldsymbol{n} \tag{17}$$

where,

$$k_1 = \frac{e^{-\sqrt{k}r}\left(e^{\sqrt{k}r}\left(k\left(a\sqrt{k}+3\right)\left(a^2+3r^2\right)-6\lambda\left(a\sqrt{k}-kr^2+1\right)\right)+6\lambda e^{a\sqrt{k}}\left(kr^2+\sqrt{k}r+1\right)\right)}{4kr^3\left(a\sqrt{k}+3\lambda+3\right)} \tag{18}$$

$$k_2 = \frac{e^{-\sqrt{k}r}\left(3e^{\sqrt{k}r}\left(-k\left(a\sqrt{k}+3\right)\left(a^2-r^2\right)+2\lambda\left(3a\sqrt{k}+kr^2+3\right)\right)-6\lambda e^{a\sqrt{k}}\left(kr^2+3\sqrt{k}r+3\right)\right)}{4kr^3\left(a\sqrt{k}+3\lambda+3\right)} \tag{19}$$

$$k_3 = \frac{e^{-\sqrt{k}r}\left(e^{\sqrt{k}r}\left(a^3k^{3/2}+3a^2k+3a\sqrt{k}\left(kr^2+2\right)+3k(2\lambda+3)r^2+6\right)-6e^{a\sqrt{k}}\left(kr^2+\sqrt{k}r+1\right)\right)}{4kr^3\left(a\sqrt{k}+3\lambda+3\right)} \tag{20}$$

$$k_4 = \frac{3e^{-\sqrt{k}r}\left(e^{\sqrt{k}r}\left(a^3\left(-k^{3/2}\right)-3a^2k+a\sqrt{k}\left(kr^2-6\right)+k(2\lambda+3)r^2-6\right)+2e^{a\sqrt{k}}\left(kr^2+3\sqrt{k}r+3\right)\right)}{4kr^3\left(a\sqrt{k}+3\lambda+3\right)} \tag{21}$$

with $k = \frac{1+\lambda}{\lambda L_B^2}$. Using this velocity field, the drag on the sphere $\boldsymbol{F}_{drag} = \iint(\boldsymbol{\sigma}_p + \boldsymbol{\sigma}_s)\boldsymbol{.n}\ a^2\sin\theta d\theta d\phi$ is given as

$$\frac{\boldsymbol{F}_{drag}}{\boldsymbol{F}_N} = \frac{(\lambda+1)\left(\frac{a\sqrt{\frac{\lambda+1}{\lambda}}}{L_B}+2\lambda+3\right)}{\frac{a\sqrt{\frac{\lambda+1}{\lambda}}}{L_B}+3\lambda+3} \tag{22}$$

where $\boldsymbol{F}_N = (6\pi\mu_s a\boldsymbol{U})$ is the Stokes drag force on a sphere in the solvent.

The limiting forms of this expression are:

$$\lim_{\lambda\to 0}\frac{\boldsymbol{F}_{drag}}{\boldsymbol{F}_N} = 1 \tag{23}$$

$$\lim_{\lambda\to\infty}\frac{\boldsymbol{F}_{drag}}{\boldsymbol{F}_N} = \frac{2\lambda}{3}. \tag{24}$$

The first limit corresponds to the value of drag on a sphere through a pure solvent and the second limit to the drag on a spherical bubble translating through a polymer fluid (owing to Eq.15). Also,

$$\lim_{L_B\to 0}\frac{\boldsymbol{F}_{drag}}{\boldsymbol{F}_N} = (1+\lambda) \tag{25}$$

$$\lim_{L_B\to\infty}\frac{\boldsymbol{F}_{drag}}{\boldsymbol{F}_N} = 1+\frac{2\lambda}{3} \tag{26}$$

which correspond, respectively, to the mixture-like behavior of the two fluids and to a sphere moving through two independent fluids exerting additive drag forces.

For the rotating sphere, the governing equations Eq.1-2 are solved using the same procedure as before with the boundary conditions now being,

$$\boldsymbol{u}_s(r) = (\boldsymbol{\omega}\times\boldsymbol{n}) \text{ at } r = a \tag{27}$$

$$\boldsymbol{u}_s, \boldsymbol{u}_p \to 0 \text{ as } r\to\infty \tag{28}$$

$$(\boldsymbol{I} - \boldsymbol{nn})\cdot(\boldsymbol{\sigma}_p\cdot\boldsymbol{n}) = 0 \text{ at } r = a \tag{29}$$

Here, solutions of the form

$$\boldsymbol{u}_s = \boldsymbol{\omega} \times \boldsymbol{n} f_s(r) \tag{30}$$

$$\boldsymbol{u}_p = \boldsymbol{\omega} \times \boldsymbol{n} f_p(r) \tag{31}$$

$$p_p = p_s = 0 \tag{32}$$

are assumed using spherical symmetry. Using these boundary conditions, the solution is obtained as:

$$\boldsymbol{u}_s = \boldsymbol{\omega} \times \boldsymbol{n} \frac{a^3 e^{-\frac{r}{\sqrt{k}}} \left(\left(a^2 + 3a\sqrt{k} + 3k \right) \left(-e^{\frac{r}{\sqrt{k}}} \right) - 3\sqrt{k}\lambda e^{\frac{a}{\sqrt{k}}} \left(\sqrt{k} + r \right) \right)}{r^3 \left(a^2 + 3a\sqrt{k}(\lambda+1) + 3k(\lambda+1) \right)} \tag{33}$$

$$\boldsymbol{u}_p = \boldsymbol{\omega} \times \boldsymbol{n} \frac{a^3 e^{-\frac{r}{\sqrt{k}}} \left(3\sqrt{k} e^{\frac{a}{\sqrt{k}}} \left(\sqrt{k} + r \right) - \left(a^2 + 3a\sqrt{k} + 3k \right) e^{\frac{r}{\sqrt{k}}} \right)}{r^3 \left(a^2 + 3a\sqrt{k}(\lambda+1) + 3k(\lambda+1) \right)} \tag{34}$$

where $k = \left(\frac{1+\lambda}{\lambda L_B^2} \right)^{-1}$. Using this velocity field, the torque on the sphere $\boldsymbol{T}_{sph} = \iint \boldsymbol{r} \times (\boldsymbol{\sigma}_p + \boldsymbol{\sigma}_s)\, a^2 \sin\theta d\theta d\phi$ is given as:

$$\frac{\boldsymbol{T}_{sph}}{\boldsymbol{T}_N} = \frac{(\lambda+1) \left(\frac{a^2}{L_B^2} + \frac{3a\sqrt{\frac{\lambda}{\lambda+1}}}{L_B} + \frac{3\lambda}{\lambda+1} \right)}{\frac{a^2}{L_B^2} + \frac{3a\sqrt{\frac{\lambda}{\lambda+1}}(\lambda+1)}{L_B} + 3\lambda} \tag{35}$$

where $\boldsymbol{T}_N = 8\pi\mu_s a^3 \boldsymbol{\omega}$ is the torque on a sphere in the solvent. From the expression for torque, we see that:

$$\lim_{L_B \to 0} \frac{\boldsymbol{T}_{sph}}{\boldsymbol{T}_N} = 1 + \lambda \tag{36}$$

$$\lim_{L_B \to \infty} \frac{\boldsymbol{T}_{sph}}{\boldsymbol{T}_N} = 1 \tag{37}$$

consistent with the expected behavior. From Fig.1(a)-(b), we see that the drag force on a translating sphere and torque on a rotating sphere of given radius a decreases with increasing in L_B. Also note that the decrease in torque is more significant than the drop in drag for a given viscosity ratio λ.

A.1 Solutions for the case with a non-interacting polymer

To obtain solutions for the case with a non-interacting polymer fluid, we assume that the polymer fluid exists everywhere in the domain, including within the sphere. Thus, one has velocity field $\boldsymbol{u}_p^{in}$ and pressure field p_p^{in} within the sphere, which satisfy Stokes equations. We have a two-fluid medium outside the sphere which satisfy Eq.1-2. The boundary conditions for this case are given by:

$$\boldsymbol{u}_s, \boldsymbol{u}_p \to 0 \text{ as } r \to \infty \tag{38}$$

$$\boldsymbol{u}_p = \boldsymbol{u}_p^{in} \text{ at } r = a \tag{39}$$

$$\boldsymbol{u}_s = \boldsymbol{U} \text{ at } r = a \tag{40}$$

$$\boldsymbol{\sigma}_p \cdot \boldsymbol{n} = 0 \text{ at } r = a \tag{41}$$

Assuming a growing velocity and pressure field for the polymer inside the sphere, given by:

$$\boldsymbol{p}_p^{in} = c_1 \boldsymbol{U} \cdot \boldsymbol{r} \tag{42}$$

$$\boldsymbol{u}_p^{in} = \left(c_2 - \frac{c_3}{3} r^2\right) \boldsymbol{U} + \left(\frac{c_1}{2} + c_3\right) (\boldsymbol{U} \cdot \boldsymbol{r})\boldsymbol{r} \tag{43}$$

subject to $\nabla \cdot \boldsymbol{u}_p^{in} = 0$, and assuming the same form for $\boldsymbol{u}_s$, $\boldsymbol{u}_p$, p_s and p_p as in Eq.3 - 6, we can solve the above system of equations to obtain the drag force as:

$$\frac{\boldsymbol{F}_{drag}}{\boldsymbol{F}_N} = \frac{(\lambda+1)\left(\frac{a^3\sqrt{\frac{\lambda+1}{\lambda}}}{L_B^3} + \frac{a^2(2\lambda+3)}{L_B^2} + \frac{18a\lambda\sqrt{\frac{\lambda+1}{\lambda}}}{L_B} + 18\lambda\right)}{\frac{a^3\sqrt{\frac{\lambda+1}{\lambda}}}{L_B^3} + \frac{3a^2(\lambda+1)}{L_B^2} + \frac{18a\lambda\sqrt{\frac{\lambda+1}{\lambda}}}{L_B} + 18\lambda(\lambda+1)} \tag{44}$$

A similar procedure can be used to calculate the torque on a rotating sphere for this case, and it can be shown to result in the same expression as Eq.35.

B Numerical scheme for SBT with validation

The numerical approach to solve the integral equations for force strength (Eq.3.12,3.30,3.31,3.62) uses the helical phase $\psi = ks\cos\theta$, where $k = 2\pi/p$ (p is the pitch) to parameterize spatial locations as,

$$\boldsymbol{r}(\psi) = R\left[\cos\psi, \sin\psi, \psi\cot\theta\right] \tag{45}$$

so an integral equation for force strength, such as Eq.3.12, becomes:

$$\begin{aligned}\boldsymbol{U}_n =& \frac{\boldsymbol{f}_n}{4\pi(1+\lambda)} \boldsymbol{\cdot} \left[(\boldsymbol{I} + \boldsymbol{t}_n\boldsymbol{t}_n)\log 2\gamma + \frac{(\boldsymbol{I} - 3\boldsymbol{t}_n\boldsymbol{t}_n)}{2}\right] + \frac{R\Delta\psi\csc\theta}{8\pi(1+\lambda)} \sum_{m\neq n} \frac{\boldsymbol{I} + \hat{\boldsymbol{r}}_{nm}\hat{\boldsymbol{r}}_{nm}}{r_{nm}} \boldsymbol{\cdot} \boldsymbol{f}_m \\ &- \sum_{m\neq n} \frac{(\boldsymbol{I} + \boldsymbol{t}_n\boldsymbol{t}_n)}{r_{nm}} \boldsymbol{\cdot} \boldsymbol{f}_n + \mathcal{O}(\Delta\psi)\end{aligned} \tag{46}$$

where $n, m = 1, 2, 3....pN$, $\boldsymbol{r}_{nm} = \boldsymbol{r}(\psi_n) - \boldsymbol{r}(\psi_m)$ is the position vector between spatial locations, $\boldsymbol{t}_n = [-sin\theta\sin\psi_n, \sin\theta\cos\psi_n, \cos\theta]$ is the tangential unit vector at $\boldsymbol{r}_n$, and $\Delta\psi$ is the mesh size of the helical phase. Note that the equation above assumes that the slender fiber has a spheroidal cross-section $\overline{a}(s) = 2\sqrt{s(1-s)}$. For convenience, we now move to a coordinate system which is rotated with the helical phase, such that the surface velocity $\boldsymbol{U}_n$ is invariant along the helix. We use these invariant velocity components to create a linear mapping between the velocity and force per unit length, which can be evaluated for a specified helical geometry, helical axial velocity U, and rotation rate Ω to give the thrust, torque, and drag. The transformation to this rotated coordinate system is achieved by means of the rotation operator $\mathcal{R}(\psi)$ defined as:

$$\mathcal{R}(\psi) = \begin{pmatrix} \cos\psi & -\sin\psi & 0 \\ \sin\psi & \cos\psi & 0 \\ 0 & 0 & 1 \end{pmatrix} \tag{47}$$

The transformed velocity and force vectors are now denoted by

$$\boldsymbol{U}'_n = \mathcal{R}(-\psi_n)\boldsymbol{\cdot}\boldsymbol{U}_n, \quad \boldsymbol{f}'_n = \mathcal{R}(-\psi_n)\boldsymbol{\cdot}\boldsymbol{f}_n \tag{48}$$

such that $\boldsymbol{U}'_n$ is invariant along the helical filament. For a rigid helix that rotates at rate Ω and translates at speed U along its axial direction, we have

$$\boldsymbol{U}'_n = [0, \Omega\, R, U]^T \tag{49}$$

and

$$\sum_{n=1}^{pN} \boldsymbol{f}'_n R\Delta\psi \csc\theta = \left[0, \frac{T}{R}, F_z\right]^T \tag{50}$$

The integral equation (Eq.3.12) now becomes,

$$\begin{aligned} \boldsymbol{U}'_n =& \frac{\boldsymbol{f}'_n}{4\pi(1+\lambda)} \cdot \left[(\boldsymbol{I} + \boldsymbol{t}'\boldsymbol{t}') \log 2\gamma + \frac{(\boldsymbol{I} - 3\boldsymbol{t}'\boldsymbol{t}')}{2} \right] - \sum_{m\neq n} \frac{(\boldsymbol{I} + \boldsymbol{t}'\boldsymbol{t}')}{r_{nm}} \cdot \boldsymbol{f}'_n \\ &+ \frac{R\Delta\psi \csc\theta}{8\pi(1+\lambda)} \sum_{m\neq n} \frac{\mathcal{R}(\psi_m - \psi_n) + \mathcal{R}(-\psi_n)\boldsymbol{.}\hat{\boldsymbol{r}}_{nm}\hat{\boldsymbol{r}}_{nm}\boldsymbol{.}\mathcal{R}(\psi_m)}{r_{nm}} \cdot \boldsymbol{f}'_m + \mathcal{O}(\Delta\psi) \end{aligned} \tag{51}$$

where $\boldsymbol{t}' = [0, \sin\theta, \cos\theta]$ is the tangent vector invariant along the helical fiber. This results in a linear mapping between $\boldsymbol{U}'$ and $\boldsymbol{f}'$ given by

$$\begin{pmatrix} \boldsymbol{U}'_1 \\ \boldsymbol{U}'_2 \\ . \\ . \\ . \\ \boldsymbol{U}'_{pN} \end{pmatrix} = \mathcal{G}. \begin{pmatrix} \boldsymbol{f}'_1 \\ \boldsymbol{f}'_2 \\ . \\ . \\ . \\ \boldsymbol{f}'_{pN} \end{pmatrix} \tag{52}$$

For a known motion of helix $\boldsymbol{U}'_n = \boldsymbol{U}^0 = [0, \Omega\, R, U]^T$, we have:

$$\begin{pmatrix} \boldsymbol{f}'_1 \\ \boldsymbol{f}'_2 \\ . \\ . \\ . \\ \boldsymbol{f}'_{pN} \end{pmatrix} = \mathcal{G}^{-1}. \begin{pmatrix} \boldsymbol{U}^0 \\ \boldsymbol{U}^0 \\ . \\ . \\ . \\ \boldsymbol{U}^0 \end{pmatrix}. \tag{53}$$

or in simple terms,

$$\boldsymbol{\mathcal{F}} = \mathcal{G}^{-1} \cdot \boldsymbol{\mathcal{U}} \tag{54}$$

where $\boldsymbol{\mathcal{F}}$ is the unknown vector of force strengths having dimension $3pN$ and $\boldsymbol{\mathcal{U}}$ is the given velocity vector of dimension $3pN$ at each grid point on the fiber surface. The total axial hydrodynamic force F_z, and net torque T are therefore given by Eq.50, which includes the thrust and torque due to rotation and the drag due to translation of the helix.

The procedure highlighted above can be generalised to the two-fluid case, for both polymer slip and no polymer-fiber interaction scenarios. For the first case, the uniformly valid SBT equation (Eq.3.46) is used, while for the latter scenario, the SBT equation with L_B restricted to the outer region (Eq.3.62) is used for numerical calculation. In the first case, one can calculate the force strengths given by the three versions of SBT ($L_B \sim O(a)$ (Eq.3.12), $L_B \gg O(a)$ (Eq.3.30,3.35) and $a \ll L_B \ll l$ (Eq.3.42,3.45)) individually and combine the total force strengths according to Eq.3.46.

For the SBT with $L_B \sim O(a)$, the equation for (total) force strength $(\boldsymbol{f}_s + \lambda \boldsymbol{f}_p)$ is similar to the SBT equation in a single fluid case and so the equation can be discretised into the form given by Eq.54, with $\mathcal{G}$ now being a function of $h(\lambda, L_B)$ and $g(\lambda, L_B)$ given in Eq.**??**. But for the other two versions of SBT (Eq.3.30,3.35 and Eq.3.42,3.45) one has two force strengths $\boldsymbol{f}_s$ and $\boldsymbol{f}_p$ at each point on the fiber, so that the unknown vector of force strengths in Eq.53 is now of dimension $6pN$ (twice as much as the dimension of unknown vector $\boldsymbol{\mathcal{F}}$ for the single fluid case) with:

$$\overline{\boldsymbol{\mathcal{F}}} = \begin{pmatrix} \boldsymbol{f}_1^{s'} \\ \boldsymbol{f}_2^{s'} \\ . \\ . \\ . \\ \boldsymbol{f}_{pN}^{s'} \\ \boldsymbol{f}_1^{p'} \\ \boldsymbol{f}_2^{p'} \\ . \\ . \\ . \\ \boldsymbol{f}_{pN}^{p'} \end{pmatrix} = \overline{\mathcal{G}}^{-1} \cdot \begin{pmatrix} \boldsymbol{U}^0 \\ \boldsymbol{U}^0 \\ . \\ . \\ . \\ \boldsymbol{U}^0 \\ \boldsymbol{U}^0 \cdot (\boldsymbol{I} - \boldsymbol{t}'\boldsymbol{t}') \\ \boldsymbol{U}^0 \cdot (\boldsymbol{I} - \boldsymbol{t}'\boldsymbol{t}') \\ . \\ . \\ . \\ \boldsymbol{U}^0 \cdot (\boldsymbol{I} - \boldsymbol{t}'\boldsymbol{t}') \end{pmatrix} = \overline{\boldsymbol{\mathcal{U}}} \tag{55}$$

where $\overline{\mathcal{G}}$ now is given by Eq.3.30,3.35 for SBT with $L_B/a \gg O(1)$ and by Eq.3.42,3.45 for SBT with $a \ll L_B \ll l$.

B.1 Validation of the numerical scheme

We validate the numerical scheme by calculating the total forces and torque on a helical fiber held in a uniform flow of a single Newtonian fluid and compare the results with those given by Johnson (1980). In his work, the author considers a helical fiber (with spheroidal cross-section) of length $l = 5p$, (where p is the pitch of the helix), radius $R_{Helix} = 0.25p$ and cross-section radius at the mid-point $a = 0.01p$, that rotates due to an external torque and translates with a velocity such that the helix is force-free. We have considered the same case and have calculated the force strength along the fiber centerline. Johnson (1980) calculates the force strength in a local coordinate system along the centerline, where the coordinate directions are tangent, normal and binormal to the centerline. We can calculate the same by using a simple coordinate transformation from our local helical coordinate system. The results from our calculation are plotted against the predictions of Johnson (1980) in Fig.1, and we see that our numerical implementation works well for fibers with curved centerline as well.

C Slender-body theory for slipping polymer with L_B in the matching region

To derive the slender-body equation with screening length in the matching region, we divide the domain into inner, outer and Brinkman regions as shown in Fig.4. In the inner region, two independent fluids undergo two-dimensional flow relative to an infinite cylinder. In the outer region, the solvent and polymer move with the same three-dimensional mixture velocity due to the distribution of singularities along the centerline. In the Brinkman region, the flow is the two-dimensional

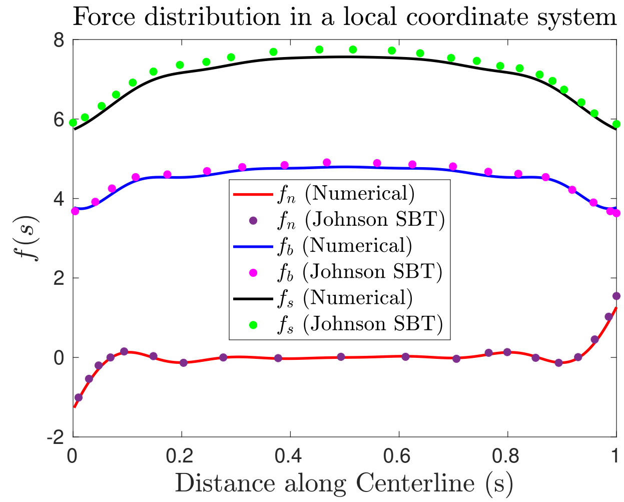

Figure 1: Comparison of the components of the force strength along the centerline of a helical fiber in a local coordinate system from our numerical implementation with the results of Johnson (1980). The helix has a prolate spheroidal cross-section with $l/p = 5$, $R_{Helix}/p = 0.25$ and $a/p = 0.01$ and undergoes force-free motion.

flow driven by a point singularity in the two-fluid medium. The dimensionless inner, outer and Brinkman solutions are given below for the solvent and polymer fluids, where the same scales used for the inner and outer region in Section 3 are used here and for the Brinkman region the length is non-dimensionalised by L_B, while the other scales are kept the same.

C.1 Inner region

For the solvent, the inner solution in the limit of $\rho/a \gg 1$ is given by:

$$\boldsymbol{u}_s^{in} = \boldsymbol{U} - \frac{\boldsymbol{f}_s \cdot (\boldsymbol{I} + \boldsymbol{e_z e_z})}{4\pi} \log \rho + \frac{\boldsymbol{f}_s}{4\pi} \cdot \left[\boldsymbol{nn} - \frac{\boldsymbol{I} - \boldsymbol{e_z e_z}}{2} \right] + O(\frac{1}{\rho^2}) \tag{56}$$

and for the polymer, one has

$$\boldsymbol{u}_p^{in} = \boldsymbol{U} \cdot (\boldsymbol{I} - (1-c)\boldsymbol{e_z e_z}) - \frac{\boldsymbol{f}_p \cdot (\boldsymbol{I} - \boldsymbol{e_z e_z})}{4\pi} \log \rho + \frac{\boldsymbol{f}_p}{4\pi} \cdot [\boldsymbol{nn} - (\boldsymbol{I} - \boldsymbol{e_z e_z})] + O(\frac{1}{\rho^2}) \tag{57}$$

C.2 Outer region

In the outer region, the solvent and polymer flow with the same velocity (the velocity of mixture) due to the distribution of singularities along the fiber centerline. The inner limit of the outer solution ($\rho/l \ll 1$) for the solvent and polymer are therefore:

$$\begin{aligned}
&\boldsymbol{u}_s^{out}(\boldsymbol{r_c}(s)) = \boldsymbol{u}_p^{out}(\boldsymbol{r_c}(s)) = \boldsymbol{U}_\infty(\boldsymbol{r_c}(s)) + \frac{\boldsymbol{f} \cdot (\boldsymbol{I} + \boldsymbol{e_z e_z})}{4\pi(1+\lambda)} \left(\log \left(\frac{2(\sqrt{s(1-s)})}{\rho} \right) \right) - \frac{\boldsymbol{f} \cdot \boldsymbol{e_z e_z}}{4\pi(1+\lambda)} + \\
&\frac{\boldsymbol{f}.\boldsymbol{nn}}{4\pi(1+\lambda)} + \frac{1}{8\pi(1+\lambda)} \int_{\boldsymbol{r_c}(s')} \left[\left(\frac{\boldsymbol{I}}{|\boldsymbol{r_c}(s) - \boldsymbol{r_c}(s')|} + \frac{(\boldsymbol{r_c}(s) - \boldsymbol{r_c}(s'))(\boldsymbol{r_c}(s) - \boldsymbol{r_c}(s'))}{|\boldsymbol{r_c}(s) - \boldsymbol{r_c}(s')|^3} \right) \cdot \boldsymbol{f}(\boldsymbol{r_c}(s')) \right. \\
&\left. - \left(\frac{(\boldsymbol{I} + \boldsymbol{e_z e_z})}{|s - s'|} \right) \cdot \boldsymbol{f}(\boldsymbol{r_c}(s)) \right] ds'
\end{aligned} \tag{58}$$

where $\boldsymbol{f} = \boldsymbol{f}_s + \lambda \boldsymbol{f}_p$.

C.3 Brinkman region

In the Brinkman region ($a \ll L_B \ll l$), the solvent and polymer are coupled by the two-fluid equations, and the flow is the two-dimensional flow driven by a point singularity. Thus, the dimensionless solvent and polymer velocity fields are:

$$\begin{aligned} \boldsymbol{u}_s^{Br} &= \boldsymbol{f}_s \cdot \boldsymbol{G}_{SS} + \lambda \boldsymbol{f}_p \cdot \boldsymbol{G}_{PS} + c_1 \\ &= \boldsymbol{f}_s \cdot \boldsymbol{G}_{St} + \frac{\lambda}{1+\lambda} (\boldsymbol{f}_s - \boldsymbol{f}_p) \cdot [\boldsymbol{G}_{Br} - \boldsymbol{G}_{St}] + c_1 \end{aligned} \tag{59}$$

$$\begin{aligned} \boldsymbol{u}_p^{Br} &= \boldsymbol{f}_s \cdot \boldsymbol{G}_{SP} + \lambda \boldsymbol{f}_p \cdot \boldsymbol{G}_{PP} + c_2 \\ &= \boldsymbol{f}_p \cdot \boldsymbol{G}_{St} + \frac{1}{1+\lambda} (\boldsymbol{f}_p - \boldsymbol{f}_s) \cdot [\boldsymbol{G}_{Br} - \boldsymbol{G}_{St}] + c_2 \end{aligned} \tag{60}$$

where c_1 and c_2 are arbitrary constants which will be determined by matching, and

$$\boldsymbol{G}_{St} = \frac{1}{4\pi} \left((\boldsymbol{I} + \boldsymbol{e_z e_z}) \log{(1/\rho)} + \boldsymbol{nn} \right) \tag{61}$$

and

$$\boldsymbol{G}_{Br} = \frac{1}{4\pi} \left((\boldsymbol{I} - \boldsymbol{e_z e_z}) A_1 \left(\rho/L_B\right) + \boldsymbol{nn} A_2 \left(\rho/L_B\right) + 2\, K_0(\rho/L_B) \boldsymbol{e_z e_z} \right) \tag{62}$$

where,

$$A_1(\chi) = 2\left(K_0(\chi) + \frac{K_1(\chi)}{\chi} - \frac{1}{\chi^2} \right) \tag{63}$$

$$A_2(\chi) = 2\left(-K_0(\chi) - \frac{2K_1(\chi)}{\chi} + \frac{2}{\chi^2} \right) \tag{64}$$

with K_ν being the modified Bessel function of order ν. Here, the length (ρ) is non-dimensionalised with L_B. The solution in the Brinkman region should be matched to both the inner and outer solution in order to obtain the SBT equation for $\boldsymbol{f}_s$ and $\boldsymbol{f}_p$. Thus in this procedure, one has two matching conditions, instead of one. In the first matching, the Brinkman solution in the limit of $\rho/L_B \ll 1$ is matched with the outer limit ($\rho/a \gg 1$) of the inner solution. This yields,

$$\begin{aligned} \boldsymbol{U} = c_1 &+ \frac{\boldsymbol{f}_s \cdot (\boldsymbol{I} + \boldsymbol{e_z e_z})}{4\pi} \log\left(\frac{L_B}{a}\right) + \frac{\boldsymbol{f}_s \cdot (\boldsymbol{I} - \boldsymbol{e_z e_z})}{8\pi} \\ &+ \frac{\lambda}{4\pi(1+\lambda)} (\boldsymbol{f}_s - \boldsymbol{f}_p) \cdot \left[(\boldsymbol{I} + \boldsymbol{e_z e_z}) \left[-\Gamma + \log 2 \right] - \frac{(\boldsymbol{I} - \boldsymbol{e_z e_z})}{2} \right], \end{aligned} \tag{65}$$

and

$$\begin{aligned} \boldsymbol{U} \cdot (\boldsymbol{I} - (1-c) \boldsymbol{e_z e_z}) = c_2 &+ \frac{\boldsymbol{f}_p}{4\pi} \log\left(\frac{L_B}{a}\right) + \frac{\boldsymbol{f}_p}{4\pi} \cdot (\boldsymbol{I} - \boldsymbol{e_z e_z}) + \\ &+ \frac{(\boldsymbol{f}_p - \boldsymbol{f}_s)}{4\pi(1+\lambda)} \cdot \left[(\boldsymbol{I} + \boldsymbol{e_z e_z}) \left[-\Gamma + \log 2 \right] - \frac{(\boldsymbol{I} - \boldsymbol{e_z e_z})}{2} \right]. \end{aligned} \tag{66}$$

Here the term with $\log(L_B/a)$ arises because the lengths are non-dimensionalised with a and L_B in the inner and Brinkman region respectively. For the second matching, the Brinkman solution in the limit of $\rho/L_B \gg 1$ should be matched with the inner limit ($\rho/l \ll 1$) of the outer solution. The resulting equations in this case are:

$$
\begin{aligned}
c_1 &= \boldsymbol{U}_\infty + \frac{\boldsymbol{f}_s + \lambda \boldsymbol{f}_p}{4\pi(1+\lambda)} \left[\log(2\gamma) + \log\left(\frac{\sqrt{s(1-s)}}{\overline{a}(s)} \right) \right] + \frac{\boldsymbol{f}_s + \lambda \boldsymbol{f}_p}{4\pi(1+\lambda)} \log\left(\frac{a}{L_B} \right) - \frac{(\boldsymbol{f}_s + \lambda \boldsymbol{f}_p) \cdot \boldsymbol{e_z e_z}}{4\pi(1+\lambda)} \\
&+ \frac{1}{8\pi(1+\lambda)} \int_{\boldsymbol{r_c}(s')} \left[\left(\frac{\boldsymbol{I}}{|\boldsymbol{r_c}(s) - \boldsymbol{r_c}(s')|} + \frac{(\boldsymbol{r_c}(s) - \boldsymbol{r_c}(s'))(\boldsymbol{r_c}(s) - \boldsymbol{r_c}(s'))}{|\boldsymbol{r_c}(s) - \boldsymbol{r_c}(s')|^3} \right) \cdot (\boldsymbol{f}_s + \lambda \boldsymbol{f}_p)(\boldsymbol{r_c}(s')) \right. \\
&\left. - \left(\frac{(\boldsymbol{I} + \boldsymbol{e_z e_z})}{|s - s'|} \right) \cdot (\boldsymbol{f}_s + \lambda \boldsymbol{f}_p)(\boldsymbol{r_c}(s)) \right] ds'
\end{aligned}
\tag{67}
$$

and

$$
\begin{aligned}
c_2 &= \boldsymbol{U}_\infty + \frac{\boldsymbol{f}_s + \lambda \boldsymbol{f}_p}{4\pi(1+\lambda)} \left[\log(2\gamma) + \log\left(\frac{\sqrt{s(1-s)}}{\overline{a}(s)} \right) \right] + \frac{\boldsymbol{f}_s + \lambda \boldsymbol{f}_p}{4\pi(1+\lambda)} \log\left(\frac{a}{L_B} \right) - \frac{(\boldsymbol{f}_s + \lambda \boldsymbol{f}_p) \cdot \boldsymbol{e_z e_z}}{4\pi(1+\lambda)} \\
&+ \frac{1}{8\pi(1+\lambda)} \int_{\boldsymbol{r_c}(s')} \left[\left(\frac{\boldsymbol{I}}{|\boldsymbol{r_c}(s) - \boldsymbol{r_c}(s')|} + \frac{(\boldsymbol{r_c}(s) - \boldsymbol{r_c}(s'))(\boldsymbol{r_c}(s) - \boldsymbol{r_c}(s'))}{|\boldsymbol{r_c}(s) - \boldsymbol{r_c}(s')|^3} \right) \cdot (\boldsymbol{f}_s + \lambda \boldsymbol{f}_p)(\boldsymbol{r_c}(s')) \right. \\
&\left. - \left(\frac{(\boldsymbol{I} + \boldsymbol{e_z e_z})}{|s - s'|} \right) \cdot (\boldsymbol{f}_s + \lambda \boldsymbol{f}_p)(\boldsymbol{r_c}(s)) \right] ds'
\end{aligned}
\tag{68}
$$

Substituting Eq.67,68 in Eq.65 and 66 gives us Eq.3.42,3.43 respectively.

References

Johnson, R.E. 1980 An improved slender-body theory for Stokes flow., *J. Fluid Mech.*, **99**(2), 411-431.